Sulfonated Polyimide Membranes for Polymer Electrolyte Fuel Cell

Ken-ichi Okamoto

Department of Advanced Materials Science & Engineering, Faculty of Engineering, Yamaguchi University, 2-16-1 Tokiwadai, Ube, Yamaguchi 755-8611, Japan

ABSTRACT

Two types of sulfonated polyimides (SPIs) (main-chain-type and side-chain-type) were prepared from 1,4,5,8-naphthalenetetracarboxiylic dianhydride, sulfonated diamines such as 4,4'-bis(4-aminophenoxy)biphenyl-3,3'-disulfonic acid, 2,2'-bis(3-sulfopropoxy)benzidine, 3,3'-bis(3-sulfopropoxy)benzidine and nonsulfonated diamines. Branched/crosslinked SPIs were also prepared from the SPI oligomers terminated by anhydride groups using 1,3,5-tris(4-aminophenoxy)benzene as a branching agent. Membrane morphology, water vapor sorption, water stability and dimensional change, proton conductivity and methanol permeability of these SPI membranes were investigated. The resulting SPI membranes displayed high proton conductivities comparable to those of Nafion 117 at high relative humidity above 80%. They displayed excellent water durability and different dimensional change based on the membrane morphology. Most of the SPIs showed much lower methanol permeabilities than Nafion membrane. Fuel cells with the SPI membranes showed excellent polarization performance, which was a little better than that for Nafion 112. The SPI membranes are expected to have great potential for polymer electrolyte fuel cell or direct methanol fuel cell applications

1. Introduction

Polymer electrolyte fuel cell (PEFC) has been developed as a promising alternative for energy conversion utilized for portable or stationary applications[1, 2]. Perfluorosulfonated polymer electrolyte membranes such as Nafion have been practically employed for PEFCs due to their excellent chemical and mechanical stability, as well as high proton conductivity [3]. However, these membranes suffer from high cost, low operating temperature and high methanol permeability. The high fluorine content also makes them difficult for post treatment. Many nonfluorinated membrane materials favorable for PEFC or direct methanol fuel cell (DMFC) applications are greatly desired. Sulfonated polyimide (SPI) is one of the most promising polymer electrolyte materials and is under active research [4-9].

Aromatic polyimides are known to have excellent thermal stability, high mechanical strength and modulus. They also have good film forming ability and superior solvent-resistance because of the strong charge transfer interaction between polymer chains. These merits of polyimides are just what are required for polymer electrolyte membranes. The initially developed SPIs with five-membered imido-rings generally showed poor stability towards acidic water due to the ease of hydrolysis of imido-rings. Mercier et al. developed six-membered imido-ring SPIs from 1,4,5,8-naphthalenetetracarboxylic dianhydride (NTDA) and reported their good stability towards acidic water. However, the NTDA-based SPIs from 2,2'-benzidinedisulfonic acid (BDSA) are still not satisfactorily stable toward water. Recently, we developed a series of novel NTDA-based SPIs with both high proton conductivity and excellent water stability from several novel sulfonated diamines. In this work, we report their water vapor sorption behavior, water stability, proton conductivity and methanol permeability and PEFC performance.

2. Synthesis and membrane formation of SPIs

According to the position of sulfonic acid group, SPIs can be classified into two types. One is noted as main-chain-type, with sulfonic groups directly bonded to the polymer backbone; the other is distinguished as side-chain-type, with sulfonic groups attached to the polymer side chains. The chemical structure of typical main-chain-type and side-chain-type SPIs is shown in Figure 1. First, sulfonated diamines such as 4,4'-bis(4-amino-phenoxy)biphenyl-3,3'-disulfonic acid (BAPBDS), 2,2'-bis(3-sulfopropoxy)benzidine (2,2'-BSPB) and 3,3'-bis(3-sulfopropoxy)benzidine (3,3'-BSPB) were prepared. Secondly, linear-type SPIs were synthesized from NTDA, sulfonated diamines and nonsulfonated diamines via one-step method in *m*-cresol in the presence of triethylamine and benzoic acid. SPI membranes were prepared by casting their *m*-cresol solutions onto glass plates and then washed with methanol, followed by proton exchange treatment with 0.5 M sulfuric acid for more than 24 h. The proton-exchanged membranes were washed with ultra-pure water and then dried in vacuo at 150 °C for 10 h.

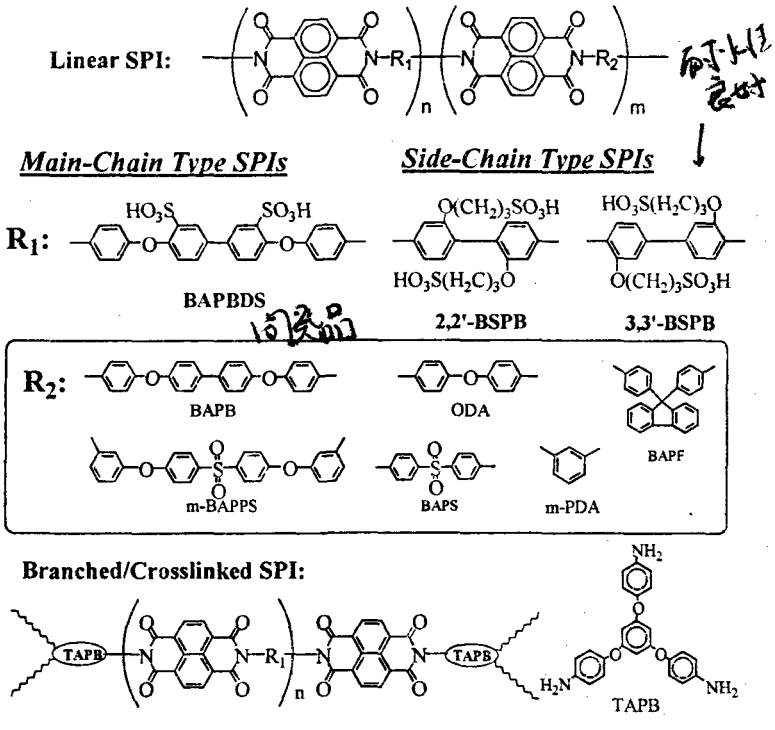

Fig. 1 Chemical structure of SPIs.

In the case of branched/crosslinked SPIs, oligomers of SPI terminated with anhydride groups were first prepared, followed by addition of 1,3,5-tris(4-aminophenoxy)benzene (TAPB), and the as-synthesized SPI solution was directly cast onto glass plate to get membranes.

3. Characterization of SPI membranes

Thermal stability of SPI membranes was investigated by TG-MS method. In the case of NTDA-2,2'-BSPB, the weight loss started at around 240 °C, which was due to the decomposition of the sulfopropoxy groups confirmed by the evolution of fragments of sulfur dioxide, propylene and propadine. The main-chain-type SPI of NTDA-BAPBDS is thermally stable up to 290 °C.

Figure 2 shows the cross-section TEM images of SPI membranes in their silver salt form. For a side-chain-type homo-SPI such as NTDA-2,2'-BSPB, a clear microphase-separated structure composed of hydrophilic sulfopropoxy groups and hydrophobic polymer backbone was formed and the ionic domains of about 5 nm connected to each other to form ionic channels. For a co-SPI, NTDA-2,2'-BSPB/BAPB(2/1), a clear microphase-separated structure was also formed, but the connection of the hydrophilic domains were rather poor compared with the homo-SPI. On the other hand, for a main-chain-type SPI such as NTDA-BAPBDS, such kind of clear microphase-separated structure was not observed.

4. Water vapor sorption

Water vapor sorption isotherms of SPI membranes are shown in Fig. 3. The number of sorbed water molecules per sulfonic group, λ, increased greatly with an increase in water vapor activity, a_w. The water vapor sorption isotherms are a comprehensive result based on the dual-mode sorption and the polymer-chain relaxation caused by sorbed water. The high water uptake at high a_w (> 0.8) is attributed to the plasticization effect of sorbed water and consequently the molecular relaxation of polymer chain. For main-chain-type SPIs, the λ - a_w relationship resembles that of Nafion in the whole a_w range. However, for side-chain-type SPIs, smaller λ values were found in the low a_w range, suggesting apparently lower Langmuir-type sorption capacity.

Apparent molar sorption enthalpy of water vapor, ΔHs, was calculated from the van't Hoff plots of solubility coefficient under a certain water vapor activity. For both main-chain-type and side-chain-type SPI membranes, with an increase in a_w, the $|\Delta Hs|$ decreased from 52 kJ/mol at a_w = 0.02 to 45 kJ/mol at a_w = 0.8, which is slightly higher than the condensation enthalpy of water vapor ΔHc (-43 kJ/mol).

The DSC curve of humidified SPI membrane was performed to investigate the ratio of freezing water and free water. In the case of water vapor activity at 0.8, the water sorbed in NTDA-BAPBDS was found to be only non-freezing water. However, for NTDA-2,2'-BSPB and Nafion 115, about 30% freezing water was found. This is probably due to the presence of hydrophilic ionic domains.

5. Water stability and membrane swelling

The water uptake (*WU*), dimensional change and water stability of SPI membranes are listed in Table 1. It is known that the water stability of SPI membranes is influenced by ion exchange capacity (IEC), *WU*, flexibility of the polymer chain, and basicity of the sulfonated diamines. Membranes with high IECs tend to yield large water uptake and thus poor water stability, and vice versa. SPIs with flexible structure and high basicity of the sulfonated diamine moieties tend to have good water stability because the flexibility allows easy molecular relaxation of polymer chain, resulting in reduction in membrane swelling stress; and the high basicity of the sulfonated diamine

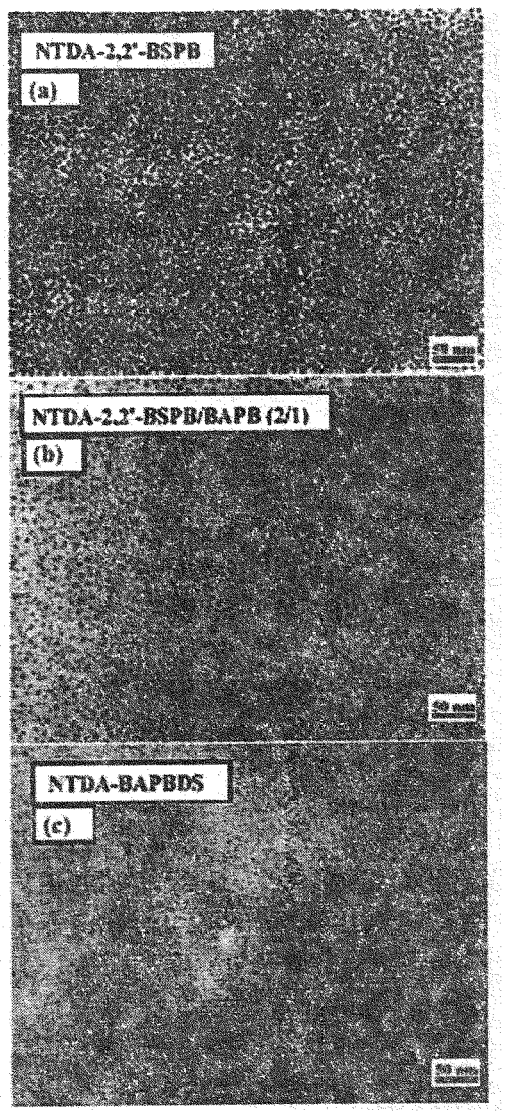

Fig. 2 TEM images of SPI membranes.

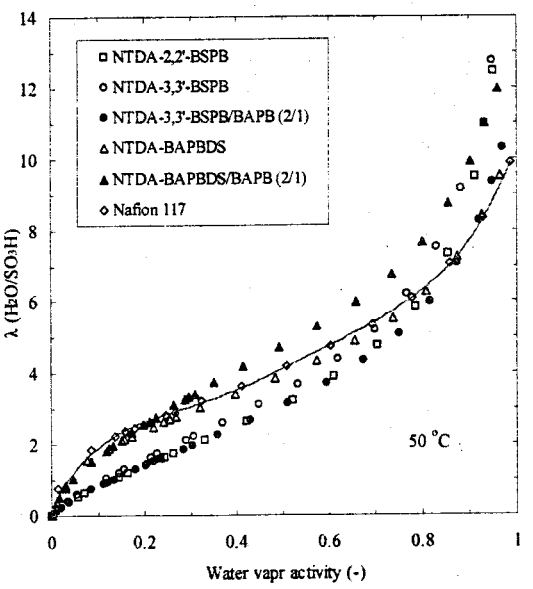

Fig. 3 Water vapor sorption isotherms of SPI membranes.

moieties depresses the hydrolysis of imido-rings. The water stability was evaluated by the elapsed time when the membrane sample began to break into pieces in water at 100 °C. The main-chain-type SPI, NTDA-BAPBDS, displayed good water stability of about 1000 h. This is attributed to the high basicity of BAPBDS and the flexible structure of polymer chain. On the other hand, co-SPIs based on 2,2'-BSPB and 3,3'-BSPB displayed much longer water stability of above 3000h. This may partly come from the higher basicity of the diamine moieties due to the electron donating effect of propoxy groups. Furthermore, the microphase-separated structure also plays an important role on their water durability. Because the hydrolysis of imid- ring is an acid-catalytic reaction, if the protons are mostly restricted in the ion-rich domains isolated from the polymer main chain, the hydrolysis of imido-ring of the SPI will be depressed.

Table 1 Water uptake, proton conductivity and dimensional change of SPI membranes.

SPIs	IEC	WU [%, g/g][a]		Conductivity [S/cm]		Dimensional change[b]	
	[meq/g]	~75%RH	in water	~75%RH	in water	Δt_c	Δl_c
NTDA-BAPBDS-No.0	2.63	26	103	0.033	0.20	0.15	0.16
No.4	2.63	—	—	0.034	0.19	0.30	0.10
No.5	2.63	—	115	0.039	0.19	0.32	0.087
No.9	2.63	—	117	0.045	0.17	0.18	0.16
NTDA-BAPBDS/BAPB(2/1)-No.5	1.89	23	93	0.019	0.13	0.28	0.078
No.8	1.89	—	80	0.020	0.14	0.41	0.086
No.11	1.89	—	88	0.026	0.13	0.35	0.065
No.14	1.89	—	51	0.019	0.11	0.20	0.044
NTDA-BAPBDS/TAPB(5/4)	2.29	—	77	0.016	0.15	0.23	0.08
NTDA-2,2'-BSPB	2.89	30	220	0.046	0.18	2.30	0.01
NTDA-2,2'-BSPB/BAPB(2/1)-No.0	2.02	—	44	0.003	0.06	0.14	0.031
No.1	2.02	—	61	0.0038	0.11	0.20	0.02
No.2	2.02	—	76	0.013	0.14	0.49	0.047
NTDA-2,2'-BSPB/BAPB(2/1)-s	2.02	—	87	0.0062	0.11	0.55	0.045
NTDA-2,2'-BSPB/TAPB(6/5)	2.42	—	104	0.011	0.14	0.59	0.01
NTDA-3,3'-BSPB	2.89	31	250	0.035	0.20	1.80	0.06
NTDA-3,3'-BSPB/BAPB(2/1)-No.1	2.02	18	62	0.0038	0.11	0.48	0.03
No.3	2.02	—	64	0.0067	0.12	0.39	0.034
NTDA-3,3'-BSPB/BAPB(2/1)-s	2.02	—	78	0.0071	0.13	0.57	0.03
NTDA-3,3'-BSPB/TAPB(5/4)	2.33	—	149	0.016	0.19	1.23	0.01
NTDA-DAPPS	2.09	23	91	0.011	0.18	0.12	0.15

[a]Measured at 50°C, [b]Measured at r.t..

The dimensional change of SPI membranes was measured at room temperature in water based on 70% relative humidity (RH) as the standard. The swelling degree was characterized by dimensional change in thickness (Δt) and diameter (Δl). Among the SPI membrane samples with the same chemical composition, the physical properties such as WU and dimensional change varied slightly or largely from batch to batch. Some slight difference in high-order structure and molecular weight of SPI and in the membrane casting conditions seemed to lead some slight difference in membrane morphology, resulting in slight or large variations in their physical properties. For a main-chain-type homo-SPI, NTDA-BAPBDS, there were observed two different types of membrane samples; one (No. 0 and 9) showed the isotropic membrane swelling with roughly equal dimensional change in thickness and in plane direction, and the other (No. 4, 5 and others) showed the anisotropic membrane swelling with much larger dimensional change in thickness than in plane. There was no large difference in WU

between these two types. For a main-chain-type co-SPI, NTDA-BAPBDS/BAPB(2/1), WU varied largely from batch to batch in the range of 51 to 93 wt%, although most of the samples showed the anisotropic membrane swelling. Side-chain-type homo-SPIs, NTDA-2,2'-BSPB and NTDA-3,3'-BSPB, had very large WU values and swelled largely only in thickness, but hardly in plane direction. Copolymerization with nonsulfonated diamines significantly reduced WU and membrane swelling in thickness, keeping the strong anisotropic membrane swelling. For NTDA-2,2'-BSPB/BAPB(2/1), WU varied largely from batch to batch in the range of 44 to 76 wt%, resulting in fairly large variations in dimensional change. The strong anisotropic membrane swelling means the presence of strong anisotropic morphology with a high degree of in-plane orientation of polyimide polymer chains in these SPI membranes.

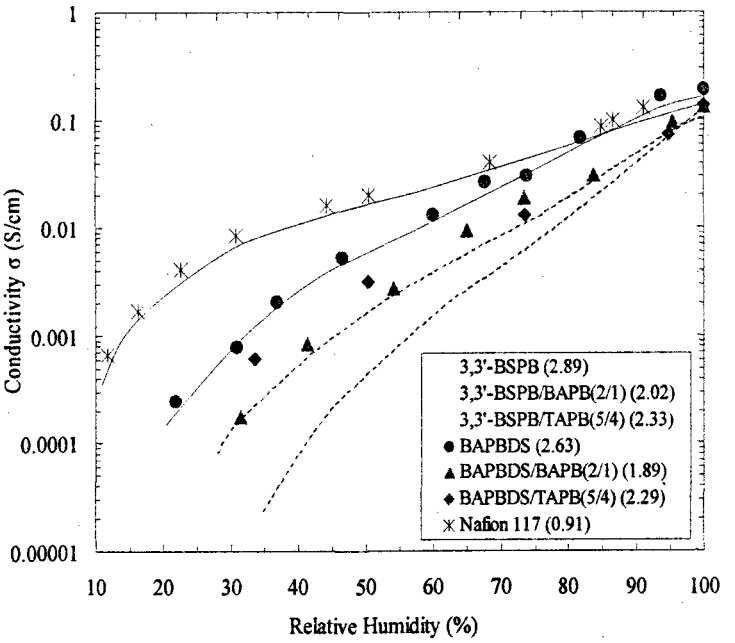

Fig. 4 Proton conductivity of NTDA-based SPI membranes at 50°C.

6. Proton conductivity

The proton conductivity in plane direction ($\sigma_{//}$) of SPI membranes is summarized in Table 1 and shown in Fig. 4 and 5 as functions of RH and temperature. The $\sigma_{//}$ values at 100% RH were measured in liquid water. It can be seen that compared with Nafion 117, the proton conductivity of SPIs displayed larger RH dependence. At RHs higher than 80%, the SPI membranes exhibited large $\sigma_{//}$ values comparable to those of Nafion.

As mentioned above, among the same SPI, WU and/or membrane swelling behavior varied fairly largely from membrane preparation batch to batch probably because of slight difference in membrane morphology. In the case of main-chain-type BAPBDS-based SPI membranes, the variation in proton conductivity was rather small. It is noted that the two types of NTDA-

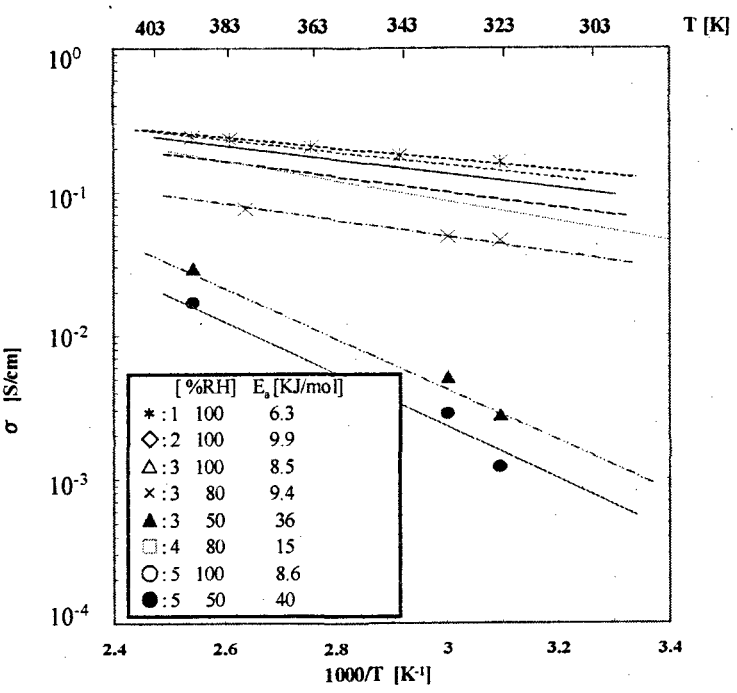

Fig. 5 Temperature dependence of proton conductivity for SPI membranes. 1:NTDA-BAPBDS 2:NTDA-BAPBDS/BAPB(2/1) 3:NTDA-BAPBDS/TAPB(5/4) 4:NTDA-2,2'-BSPB 5:NTDA-3,3'-BSPB/TAPB(5/4))

BAPBDS membrane samples with isotropic and anisotropic membrane swelling showed the similar values of $\sigma_{\parallel}$. On the other hand, in the case of side-chain-type BSPB-based co-SPI membranes, the proton conductivity varied largely from batch to batch depending on WU. This seems due to the difference in microphase-separated structure. Furthermore, it is noted that the BSPB-based co-SPI membranes had rather smaller proton conductivity than the BAPBDS-based co-SPI membranes, in spite of a little higher IEC of the fomer.

The activation energies ΔE_a of proton conductivity in water were 9-11 KJ/mol for various SPI membranes and 12 KJ/mol for Nafion 117, which were similar to the reported values for Nafion 117 (ΔE_a = 9-13 KJ/mol) and sulfonated polysulfone (ΔE_a = 10-12 KJ/mol)[10].The ΔE_a at 80%RH was in the range of 9 to 15 KJ/mol, whereas the ΔE_a at 50%RH was about 40 kJ/mol, which was much larger than that in water. Most of the SPI membranes displayed high proton conductivities of 0.1-0.05 S/cm at temperatures above 353K and at 80%RH, which is promising for PEFC applications at medium temperatures.

Table 2 Mechanical properteies of SPI membranes before and after soaking in water.

SPIs	Soaking conditions	Youngs Modulus (GPa)	Maximum Stress (MPa)	Elongation at break (%)
NTDA-BAPBDS	No treatment	1.14	54	58
	100°C, 10h	-	22	64
NTDA-BAPBDS/BAPB(2/1)	No treatment	1.22	104	126
	130°C, 24h	0.80	44	5.9
	130°C, 48h	0.81	40	5.6
	130°C, 96h	0.61	34	6.2
NTDA-BAPBDS/TAPB(5/4)	No treatment	1.22	98	78
	130°C, 48h	0.90	55	10
	130°C, 96h	0.83	57	15
NTDA-3,3'-BSPB/TAPB(6/5)	No treatment	2.30	130	18
	130°C, 48h	2.00	120	16
	130°C, 96h	1.90	110	17
	130°C, 196h	2.00	90	12

7. Water stability as for mechanical strength and proton conductivity

Mechanical properties of SPI membranes before and after soaking in water are summarized in Table 2. NTDA-BAPBDS membrane lost its mechanical strength rapidly, whereas the corresponding co-SPI, NTDA-BAPBDS(2/1) membranes kept its mechanical strength fairly well even after the soaking at 130 ℃ for 96h. We investigated the change in molecular weight for these membranes by measuring the intrinsic viscosity [η]. For NTDA-BAPBDS, the [η] decreased down to a third of the original after the soaking at 100 ℃ for 24h, but did not further decrease after 50h. The initial decrease in [η] was smaller for the co-SPI membrane. This means both imido-rings and polymer chains decomposed only in the early period of soaking, but did not decompose in the further soaking. As a result, the molecular weight of membrane was kept at a level, which was lower than the original. Molecular relaxation of polymer chains occurred simultaneously in the soaking. As a result, membrane lost its mechanical strength in a shorter time, especially for the homo-SPI. On the other hand, the membranes kept their form in much longer time, because their molecular weights were kept at a level. On the other hand, the mechanical strength was further improved for the branched/crosslinked SPI membranes because of the reduced molecular relaxation.

The elimination of sulfo and sulfopropoxy groups during the soaking in hot water was investigated by measuring a change in $\sigma_{//}$ and an elimination loss of sulfur into soaking water (S loss in mol%). With an increase in soaking time and temperature, the sulfur loss increased slightly. In the case of the BAPBDS –based SPI membranes, the S loss was less than 8 % for the soaking at 130 ℃ for 96h and the $\sigma_{//}$ hardly changed. In the case of the BSPB-based co-SPI membranes, some membranes showed low S loss and negligible change in $\sigma_{//}$, but another membranes showed rather large S loss and large reduction in $\sigma_{//}$. The large loss of S was attributed to the elimination of sulfopropoxy groups by means of the ion chromatography. Thus, the proton conductivity stability significantly depended on the membrane preparation batch and probably on the membrane morphology. Further study is necessary to improve the proton conductivity for the side-chain-type co-SPI membranes.

Table 3 Methanol permeability of SPI membranes

Membrane	IEC	σ [S/cm][a]		P_M [10^{-6} cm^2/s]		φ=σ/P_M [10^4 $Scm^{-3}s$	
	[meq/g]	303K	323K	303K[b]	323K[c]	303K[b]	323K[c]
BAPBDS No.1	2.63	0.16	0.19	1.29	2.58	14	7.4
BAPBDS/BAPB(2/1) No.1	1.86	0.11	0.14	1.05	1.19	10	12
No.6	1.86	0.08	0.10	0.40	0.76	20	13
BAPBDS/TAPB(5/4)	2.29	0.13	0.17	0.83	1.58	16	11
2,2'-BSPB/BAPB(2/1) No.0	2.02	0.05	0.06	0.66	0.51	7.6	12
No.1	2.02	0.08	0.11	1.00	2.20	8.0	5.0
2,2'-BSPB/BAPPS(2/1)	1.95	0.04	0.05	0.32	0.47	13	11
2,2'-BSPB/PDA(2/1)	2.32	0.13	0.15	1.05	1.19	12	13
3,3'-BSPB/BAPB(2/1) No.1	2.02	0.08	0.11	0.48	1.04	17	11
No.3	2.02	0.08	0.12	0.92	1.19	8.7	10
3,3'-BSPB/BAPB(2/1)-s	2.03	0.10	0.13	0.75	—	13	—
3,3'-BSPB/ODA(2/1)	2.23	0.13	0.16	1.36	1.62	9.6	9.9
3,3'-BSPB/BAPS(2/1)	2.17	0.13	0.15	1.20	1.56	11	9.6
3,3'-BSPB/BAPF(2/1)	2.04	0.09	0.11	0.52	0.87	17	13
3,3'-BSPB/BAPPS(2/1)	1.95	0.06	0.088	0.55	1.01	11	8.7
3,3'-BSPB/TAPB(6/5) No.1	2.57	0.15	0.18	1.16	1.75	13	10
3,3'-BSPB/TAPB(5/4) No.1	2.49	0.14	0.19	2.1	2.8	6.7	7.8
SPS_{20}[d]	1.41	0.05	0.086	0.52[e]	1.19[f]	9.6[e]	7.2[f]
Nafion115	0.91	0.1	0.11	2.72	3.3	3.7	3.3

[a]Measured in water. [b]Methanol concentration in feed: 30wt%. [c]Methanol concentration in feed: 10wt%.
[d]Sulfonated poly(stryrene) with sulfonation degree of 20 mol%. [e]Measured at 22°C. [f]Measured at 60°C.

8. Methanol permeation properties

Methanol permeability was measured by liquid-liquid method with feed concentrations of 10 and 30wt%. The methanol permeability (P_M), $\sigma_{//}$ and their ratio Φ (=$\sigma_{//}$ /P_M) are listed in Table 3. The data of sulfonated polystyrene with 20% sulfonation degree (SPS20) are also shown for comparison[11]. It is clearly seen that the SPIs in this study showed much lower P_M values than those of Nafion 117 and exhibited relatively high $\sigma_{//}$ values as well, under the same condition. As a result, the membrane selectivity, Φ values of SPI membranes were about 2-5 times larger than those of Nafion and SPS20, suggesting potential for DMFC. As can be seen in Table 3, among the same SPI, the P_M varied more largely from membrane preparation batch to batch than the $\sigma_{//}$. Therefore, it is important to control the membrane morphology most suitable for DMFC application.

9. Polymer electrolyte fuel cell performance

A single fuel cell performance was investigated using a membrane electrode assembly (MEA) fabricated by hot-pressing the sandwich of electrode/SPI-membrane/electrode (effective membrane area: 5cm^2). A 5wt% Nafion solution was impregnated on the catalytically active surface of the electrodes (20wt% PT/Vulcan XC-72, E-TEK Inc.) to provide a better contact with the SPI membrane. Figure 6 shows the fuel cell performances of BAPBDS-based SPIs in a H_2/O_2 system at 90°C. NTDA-BAPBDS and NTDA-BAPBDS/BAPB(2/1) membranes displayed a little better fuel cell performance than that of Nafion 112. Branched/crosslinked SPI membranes derived from BAPBDS and BPDS also displayed high performance comparable to Nafion112. The PEFC performances for these SPI membranes were much better than those for the BDSA-based SPI membranes reported by Besse et al., For example, the cell voltage with a current load of 1 A/cm^2.was 0.69 V for the present SPI membranes and 0.20-0.40 V for the BDSA-based SPI membranes.[5] This is probably due to the higher proton conductivity and the thinner thickness of the present membranes.

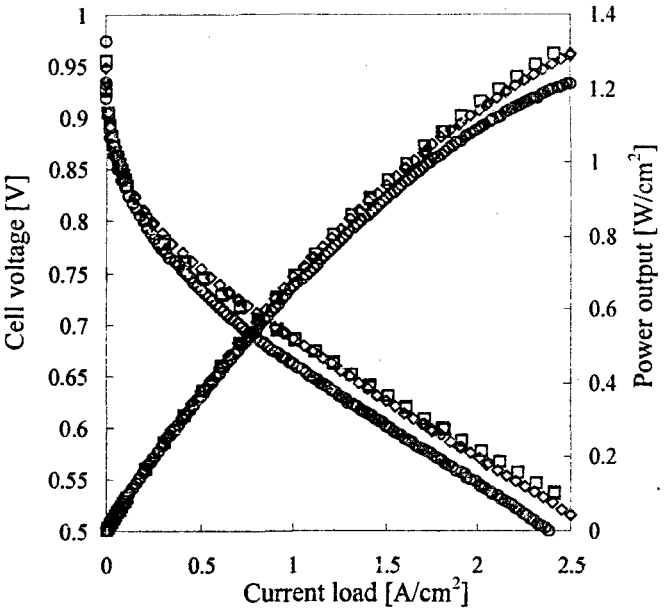

Fig. 6 Fuel cell performance of SPI membranes (Temp.: 90°C, Pressure: 0.3MPa). □:NTDA-BAPBDS(No.5), ◇:NTDA-BAPBDS/ BAPB (2/1) (No.14), ○ :Nafion112
Anode: H_2 150ml/min. (90/88 °C),
Cathode:O_2 100ml/min. (90/85 °C)

REFERENCES

1) J. A. Kerres, *J. Membr. Sci.*, **185**, 3-27 (2001).
2) K.D. Kreuer, *J. Membr. Sci.*, **185**, 29-39 (2001).
3) O. Savadogo, *J. New Mat. Electrochem. Syst.*, **1**, 47-66 (1998).
4) C. Genies, R. Mercier, B. Sillion, N. Cornet, G. Gebel, M. Pineri, *Polymer*, **42**, 359-373 (2001).
5) S. Besse, P. Capron, O. Diat, G. Gebel, F. Jousse, D. Marsacq, M. Pineri, C. Marestin, R. Mercier, *J. New Mat. Electrochem. Syst.*, **5**, 109-112 (2002).
6) J. Fang, X. Guo, S. Harada, T. Watari, K. Tanaka, H. Kita, and K. Okamoto, *Macromolecules*, **35**, 6707-6713 and 9022-9028 (2002).
7) T. Watari, J. Fang, K. Tanaka, H. Kita, K. Okamoto and T. Hirano, *J. Membr. Sci.*, **230**, 111-120 (2004).
8) Y. Yin, J. Fang, Y. Cui, K. Tanaka, H. Kita and K. Okamoto, *Polymer*, **44**, 4509-4518 (2003).
9) Y. Yin, J. Fang, T. Watari, K. Tanaka, H. Kita and K. Okamoto, *J. Mater. Chem.*, **14**, 1062-1070 (2004).
10) F. Lufrano, I. Gatto, P. Staiti, V. Antonucci and E. Passalacqua, *Solid State Ionics*, **145**, 47-51 (2001).
11) N. Carretta, V. Tricoli, F. Picchioni, *J. Membr. Sci.*, **166**, 189-197 (2000).